Ultrasonics Sonochemistry 94 (2023) 106315

Contents lists available at ScienceDirect

Ultrasonics Sonochemistry

journal homepage: www.elsevier.com/locate/ultson

Ultrasound-enhanced interfacial adsorption and inactivation of soy trypsin inhibitors

Yue Wu [a], Wu Li [b], Haiyan Zhu [a], Gregory J.O. Martin [b,*], Muthupandian Ashokkumar [a,*]

[a] Sonochemistry Group, School of Chemistry, The University of Melbourne, Parkville, Victoria 3010, Australia
[b] Algal Processing Group, Department of Chemical Engineering, The University of Melbourne, Parkville, Victoria 3010, Australia

ARTICLE INFO

Keywords:
Soy trypsin inhibitors
Liquid–liquid interface
Ultrasound
Inactivation
Oil type

ABSTRACT

In this study, liquid–liquid interfacial protein adsorption was proposed as a means of inactivating soy trypsin inhibitors (TIs, including Kunitz (KTI) and Bowman-Birk inhibitor (BBI)). Hexane-water was first selected as a model system to compare three emulsification methods (hand shaking, rotor–stator and ultrasound mixing). Ultrasound could generate the smallest and least polydisperse emulsion droplets, resulting in highest interfacial adsorption amount of KTI and BBI as well as the highest inactivation percentage of TIs ($p < 0.05$). Therefore, ultrasound was selected to further explore the effect of the non-aqueous phase on interfacial adsorption and inactivation kinetics of TIs in a food emulsion system containing vegetable oil (VTO). The adsorption amounts of KTI and BBI in the VTO-aqueous emulsion increased by ~ 25 % compared to the hexane-aqueous emulsion. In addition, the adsorption amounts of KTI and BBI were rapidly increased as a function of sonication time, especially for the hexane-aqueous emulsion system. This result suggests that such inactivation of TIs could be implemented in continuous systems for large-scale processing. Finally, the pathways of interface-induced inactivation of BBI and KTI were investigated based on separate experiments on individual BBI and KTI systems. The results showed that the interface adsorption caused the changes in the secondary and tertiary structure of KTI that led to its activitation. However, BBI was quite stable at the liquid–liquid interface without significant conformational change. Overall, ultrasound-assisted interfacial adsorption can be considered a rapid and highly efficient method to inactivate KTI.

1. Introduction

The continued increase in human population contributes to more demand for plant-based products and meat alternatives, especially for some vegans or vegetarians [1]. Compared with other plant-based products, soy products attracted more interest due to their low-fat content, high protein content, low price and product diversification [2]. However, the presence of anti-nutritional compounds in soy products limits their consumption [3]. Trypsin inhibitors (TIs) are the typical anti-nutritional serine protease enzymes that are found in soy products [4,5]. Up to now, two different trypsin inhibitors, namely Kunitz inhibitor (KTI) and Bowman-Birk inhibitor (BBI), have been identified [5]. Kunitz inhibitor is a stable monomeric, non-glycosylated and globulin-type protein with a molecule weight of 20 kDa [6]. In comparison, Bowman-Birk has a rigid structure stabilised by seven disulphide bonds, with a smaller molecule weight of 10 kDa [7]. Both BBI and KTI are undesirable because they can inhibit the activity of some important digestive proteases (e.g., trypsin and chymotrypsin) [8]. The uptake of BBI, KTI and TIs can impair protein digestibility and absorption as well as increase pancreatic secretory activity [9]. Therefore, the inactivation of TIs is vital to acquire soy products with better nutritional quality.

Recently, various traditional and advanced processes have been applied to inactivate KTI and BBI [5,8–10]. Many of these inactivation processes require high temperature (e.g., 200 °C) [11], high pressures (i.e., 600 MPa) [12], extreme pH conditions (<2 and > 10) [13] or extended treatment times (>30 mins) [8,10], all of which can increase cost and damage other nutritional components. Accordingly, it is important to find new methods to inactivate TIs that are effective, efficient, and don't require these extreme conditions. The simultaneous interfacial adsorption could be a potential approach to alter the

Abbreviations: Trypsin inhibitors, TIs; Bowman-Birk inhibitor, BBI; Kunitz inhibitor, KTI; Untreated trypsin inhibitors, UNTI; Hand shaking, HS; ULTRA-TURRAX, UT; Ultrasound, US; Vegetable oil, VTO.

* Corresponding authors.
E-mail addresses: gjmartin@unimelb.edu.au (G.J.O. Martin), masho@unimelb.edu.au (M. Ashokkumar).

https://doi.org/10.1016/j.ultsonch.2023.106315
Received 18 November 2022; Received in revised form 24 January 2023; Accepted 29 January 2023
Available online 2 February 2023

biological functions of proteins without involving chemicals or extreme physical conditions [14–17]. To be specific, proteins can be adsorbed to the solid–liquid, liquid–liquid and liquid–gas interface due to their amphiphilic structure and then undergo continuous changes in their shape or conformation [14,15]. As a result, these conformational changes may help to inactivate biological functions originated from the native protein structure [16,17]. Such adsorption procedure has been commonly studied with food proteins [17–19], and is ultimately influenced by the interfacial properties (e.g., types of liquid pairs) [17,19] and the physicochemical properties of proteins (e.g., the structure of proteins) [18]. For instance, Lefevre and Miller [17,19] indicated that the adsorbed β-lactoglobulin undergoes an irreversible change in secondary structure at a water–oil interface while it can be slowly desorbed from a water–air interface of a Langmuir trough by exchanging the subphase with pure water. Bergfreund et al. [18] demonstrated that the adsorption rate of random-coil proteins (β-casein) was faster than globular proteins (egg white lysozyme) at water-MCT (medium chain triglycerides) interface. Accordingly, interfacial adsorption can be considered a potential method to inactivate TIs by disrupting their native conformation. However, to our best knowledge, this approach has yet to be applied to the inactivation of TIs. In addition, there is limited knowledge about the conformational changes of KTI and BBI at the interface with different properties.

Interface between two immiscible liquids widely exists in the food industry from the upstream processing to the final products [20,21], and can be easily manipulated by established emulsification and demulsification processes [22]. Generally, the emulsification process requires emulsification methods with high turbulence intensity [22–24], low interfacial tension [24], suitable process time [25,26] and emulsifiers [27]. For example, Taha et al. [24] found that the droplet size of soy protein-palm oil emulsions prepared by ultrasound was 10 times smaller than that prepared by high-shear homogenization, which contributed to a higher adsorption amount of soy proteins. Ma et al. [27] reported that the cod proteins modified by ultrasound as an emulsifier has higher stability of emulsions with a 50 % increase in adsorption amount compared to the native one. Additionally, it has been reported that medium-chain triglycerides produced emulsions with smaller droplets and higher protein adsorption than long-chain triglycerides in oil-in-water emulsions stabilized by soy protein isolate [24]. However, little is known about the effect of emulsification methods and properties of the non-aqueous phase liquids on the adsorption and inactivation of TIs.

In this study, the feasibility and mechanism of inactivation of KTI and BBI using liquid–liquid interfacial adsorption were systematically evaluated in both individual KTI and BBI solutions and in mixtures of the two. Firstly, a model emulsion system containing hexane and an aqueous TI mixture was developed to verify the possibility of interface-induced inactivation of TIs. The effect of turbulent conditions was examined with hand shaking, rotor–stator mixing and ultrasonication on the basis of interfacial area, adsorption and inactivation amount of TIs. Next, ultrasound-assisted interfacial inactivation was investigated in a food emulsion system (vegetable oil–water) to examine the effect of non-aqueous phase types and the adsorption kinetic of TIs. Finally, the interfacial-induced inactivation was examined in individual inhibitor systems to elaborate their different individual adsorption behaviour at water–oil interfaces, associated with the conformational characterizations during the interfacial adsorption. Overall, this research proposed a novel approach and its mechanism of TIs inhibition for the food industry without the use of extreme temperature, pressure or pH.

2. Materials and methods

2.1. Materials

KTI standard (Cat No. T2327, purity > 95 %), BBI standard (Cat No. T9777, purity > 90 %), lyophilised powder of TIs (contains KTI and BBI, Cat No. T9128, purity > 60 %), Nα-Benzoyl-DL-arginine 4-nitroanilide hydrochloride (BApNA) and trypsin from porcine pancreas (Type II-S) were all purchased from Sigma-Aldrich (St Louis, MO, USA) and stored at 4 °C until use. Vegetable oil (VTO) was bought from a local supermarket in Melbourne, Australia. 4–20 % Criterion™ TGX™ Precast PAGE Gels were purchased from Bio-Rad Laboratories (Gladesville, NSW, Australia) and stored at 4 °C. Chemicals including *n*-hexane (HPLC-grade, purity > 99.99 %), hydrochloric acid (HCl, 36 %), trifluoroacetic acid (TFA, HPLC-grade, purity > 99.99 %), acetonitrile (HPLC-grade, purity > 99.99 %) were purchased from Sigma-Aldrich and stored at room temperature (20 °C). All materials and chemicals were used directly without further purification. Deionised water was acquired from a Millipore RiOs/Origin system (Millipore Australia Pty ltd., NSW, Australia) with a resistivity of 18 mΩ cm.

2.2. Interfacial adsorption and inactivation of TIs

2.2.1. Adsorption of TIs at a hexane-water interface under different emulsification methods

To investigate the feasibility of interface-induced inactivation of TIs, hexane-water system was chosen as a model because the adsorbed TIs can be easily collected by volatilizing the hexane. In addition, hexane has been used to investigate the adsorption behaviour of proteins at the interface [28]. Three different emulsification methods, including hand shaking (HS), rotor–stator mixing (ULTRA-TURRAX, UT) and power ultrasound (US) mixing were compared basis of the volume and droplet size of emulsion and the adsorption and inactivation amount of TIs. For the interfacial adsorption emulsification process, hexane was added into a TI mixture solution (containing both BBI and KTI) with a concentration ranging from 200 mg/L to 1000 mg/L at a ratio of 1:1 (v:v). Next, the two immiscible phases were emulsified by hand shaking (2 rotational cycle/second), rotor–stator mixing (13, 500 rpm, ULTRA-TURRAX, IKA, Cologne, Germany) and power ultrasound mixing (20 kHz, 1.28 W/mL, Branson, Model No. 450) for 20 s [29]. The experimental images of interfacial adsorption generated by different emulsification methods and microstructure of the emulsion layer observed using microscopy were presented in SI Fig. 1. To collect the adsorbed TI fraction from the hexane-aqueous interface, the TI-hexane emulsion (including the adsorbed and unadsorbed TIs) was collected and subjected to a 48-h freeze-drying process (Christ Alpha 1–2 LD Plus, Germany) to remove both hexane and water. The freeze-dried samples were then collected carefully and redissolved in deionised water to analyse the change in physicochemical properties. All the experiments were performed in triplicate.

2.2.2. Adsorption kinetic of TIs in a food emulsion system different non-aqueous interface

The emulsification method (US) with the highest potential on the generation of emulsion and enhancement of adsorption and inactivation of TIs was selected for further study on the effect of non-aqueous phase. Considering the actual emulsion process in the food industry, VTO is considered as the representative non-aqueous phase to reflect the efficiency of interface-induced inactivation of TIs in the practical food system [29,30]. The sonication time was set from 0 s to 240 s to provide sufficient interfacial adsorption and avoid denaturation of TIs caused by long-duration US [8,29–31]. To be detailed, the effect of non-aqueous phases and ultrasonication time were evaluated using mixed TIs solutions (1000 mg/L, containing KTI and BBI) mixed with hexane or VTO at a ratio of 1:1 (v: v). Ultrasonic emulsification was performed at 20 kHz using a Branson, Model No. 450 generator equipped with a 12 mm ultrasonic probe. For each emulsion system, 30 mL of immiscible liquids were put into a 50 mL glass container which was immersed in an ice-water bath to prevent an increase in temperature during ultrasonication. Ultrasonic was applied in pulses (5 s on, 5 s off) for 240 s at a power density of 1.38 ± 0.1 W/mL. 0.8 mL samples were collected at each time point (20 s, 40 s, 80 s, 120 s, 180 s, 240 s) for physicochemical and activity analysis [29–31]. To measure the adsorbed amount of TIs,

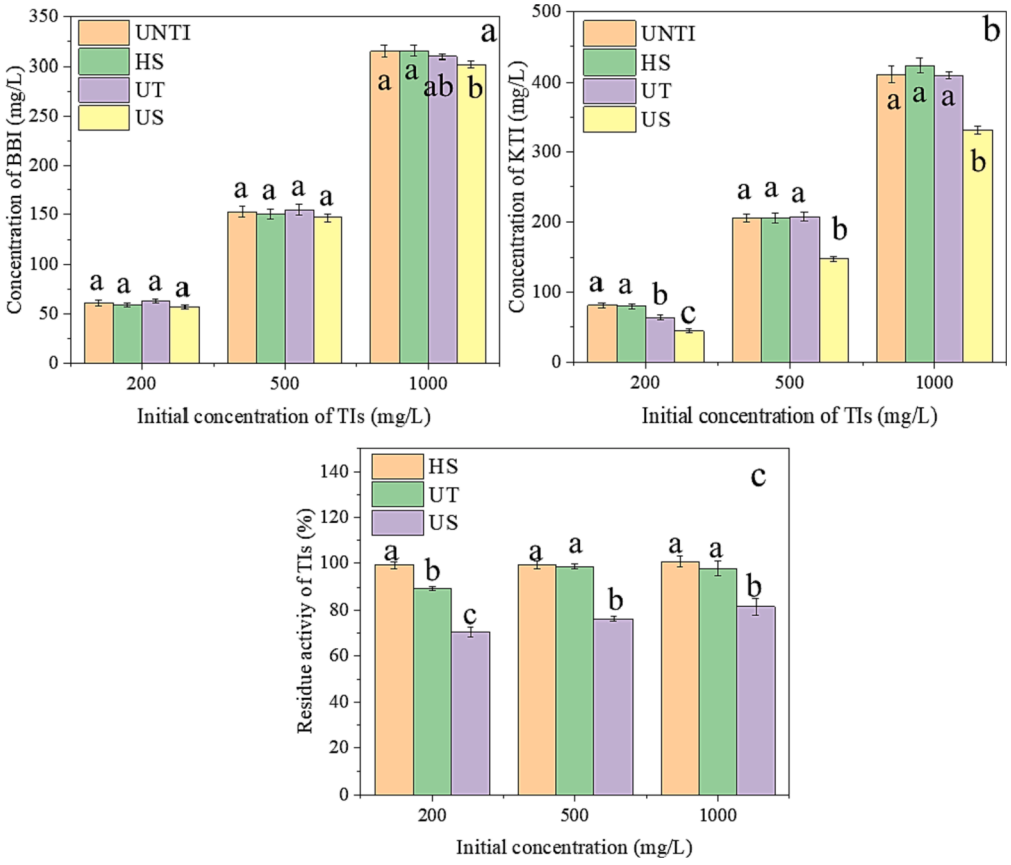

Fig. 1. The residual amount of BBI (a) and KTI (b) in the aqueous phase from hexane-TI solution (200 mg/L-1000 mg/L, ratio of 1:1 (v:v)) emulsions produced by hand shaking, ULTRA-TURRAX mixing and ultrasound mixing. The corresponding residual inhibitory activity of desorbed TIs from hexane-water interface (c). Note: UNTI: untreated soy trypsin inhibitors; HS: hand shaking; UT: ULTRA-TURRAX mixing; US: ultrasound mixing; BBI: Bowman-Birk inhibitor; KTI: Kunitz inhibitor; TIs: trypsin inhibitors (mixture of BBI and KTI). Different lowercase letters represent significant differences among different treatments ($p < 0.05$). The experiments were conducted in triplicate.

samples were centrifuged at 10, 000 g for 30 min at 25 °C in a temperature-controlled centrifuge (Allegra X-30R, Beckman Boulter, USA) to obtain the cream layer and serum layer [32,33]. Then the adsorbed TI amount can be calculated by the difference between the content of initial TI and TI in the serum layer. All the experiments were performed in triplicate.

2.3. Interfacial adsorption and inactivation of BBI and KTI

To clarify the mechanism of interfacial adsorption-induced inactivation of the individual TI, BBI and KTI standard solutions were prepared and their adsorption procedure at the VTO-water and hexane-water interface following the method described in section 2.2. Two immiscible phases consisted of VTO/hexane and BBI solution (500 mg/L) or VTO/hexane and KTI solution (500 mg/L) as the ratio of 1:1 (v:v). Then, the immiscible liquids were emulsified by ultrasonication at 20 kHz and 1.28 W/mL. To observe the change of structure and conformation of adsorbed BBI and KTI at the interface, the lyophilise power of untreated BBI/KTI and desorbed BBI/KTI after removing the hexane-water interface by freezing drying at −50 °C and under 0.04 mbar pressure for 48 h (Christ Alpha 1–2 LD Plus, Germany) was collected for the structural analysis.

2.4. The physicochemical properties of TIs

2.4.1. Quantification of individual TI content of adsorbed TIs at hexane-water and VTO-water interface

To verify whether the BBI, KTI or both can be adsorbed at the liquid–liquid interface, the amount of residue KTI and BBI was analysed using an Agilent 1260 Infinity HPLC system (Agilent Technology Company, USA) coupled with a Jupiter RP-C18 column (250 × 4.6 mm, 5 μm, 300 Å) following the method described by Wu et al [10]. The binary mobile phases were composed of (A) trifluoroacetic acid (0.1 %) in water and (B) trifluoroacetic acid (0.1 %) in acetonitrile at a flow rate of 1 mL/min. The gradient elution program was set as follows: 0–20 min: 17 % B-33 % B; 20–36 min: 33 % B-55 % B; 36–50 min: 17 % B. The column temperature and detection wavelength were 45 °C and 210 nm, respectively. 20 μL samples were injected by the HPLC autosampler. Before injection, samples were centrifuged at 10, 000 g for 30 min at 25 °C in a temperature-controlled centrifuge (Allegra X-30R, Beckman Boulter, USA) [32,33]. The aqueous phase (serum layer) was collected and filtered using 0.22 um PES filter to obtain the unabsorbed TIs [32,33]. The individual TIs (BBI and KTI) were identified according to the KTI and BBI standards (SI Fig. 2) and their concentrations were quantified by the calibration curves of the KTI and BBI standards (SI Fig. 3). The amount of interfacially adsorbed KTI and BBI was determined based on the differences between the initial concentrations and unabsorbed concentrations of KTI and BBI.

2.4.2. Determination of inhibitory activity of TIs after interfacial adsorption

To evaluate whether the interface adsorption affected trypsin inhibition activity, a colorimetric assay was used to measure the TI activity [8]. Interfacial desorbed TIs were collected from the hexane-TI emulsion and subjected to freeze drying process. TI emulsions prepared with VTO were first centrifuged and the cream layer removed priority to measure the residual activity of TIs remaining in the aqueous phase [32].

For the measurement of inhibitory activity of TIs, 40 mg of BApNA powder was first dissolved in 1 mL dimethyl sulfoxide (DMSO) and then sonicated in an ultrasonic bath for 1 min to prepare the BApNA solution. Next, this solution was diluted to 100 mL with Tris-buffer solution (0.05 M, pH 8.2) to obtain the substrate solution. For the assay reaction procedure [34], all tubes, reagents and samples were pre-heated at 37 °C for 10 min. Then 0.2 mL trypsin solution (500 mg/L) was mixed with 0.2 mL of diluted samples (50 mg/L) or deionised water (control) and incubated

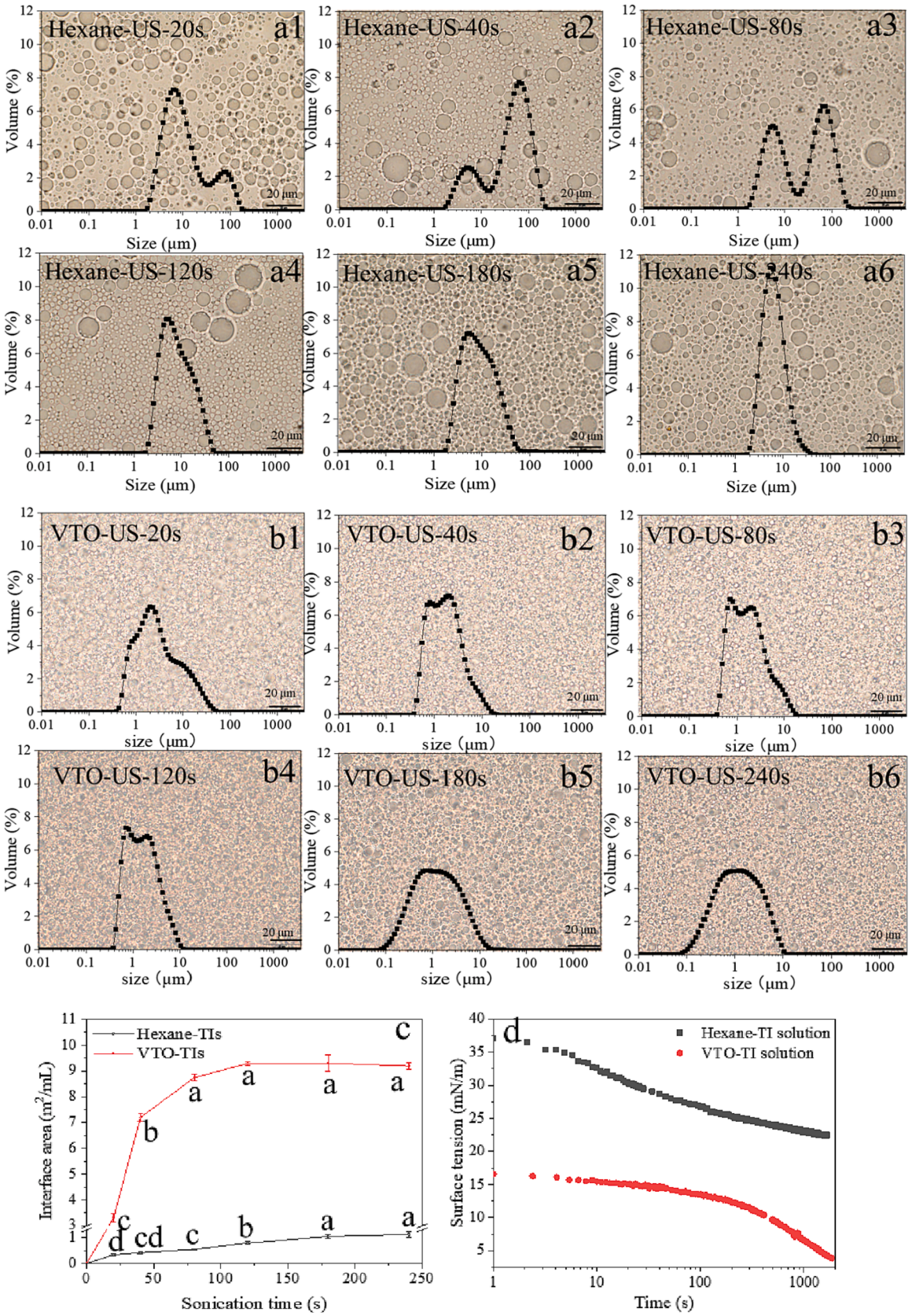

Fig. 2. Optical microscopy images (60 ×) and corresponding size distribution of hexane-TIs (1000 mg/L) (a1-a6) and VTO-TIs (1000 mg/L) (b1-b6) emulsions prepared over different sonication times (20 s-240 s). The corresponding interfacial area of hexane-TIs and VTO-TIs emulsion (c). The dynamic change of interfacial tension of TIs (1000 mg/L) at hexane-water and VTO-water interfaces (1800 s). Note: VTO: vegetable oil; US: ultrasound mixing. Different lowercase letters represent significant differences in the surface areas at different sonication times ($p < 0.05$). The experiments were conducted in triplicate.

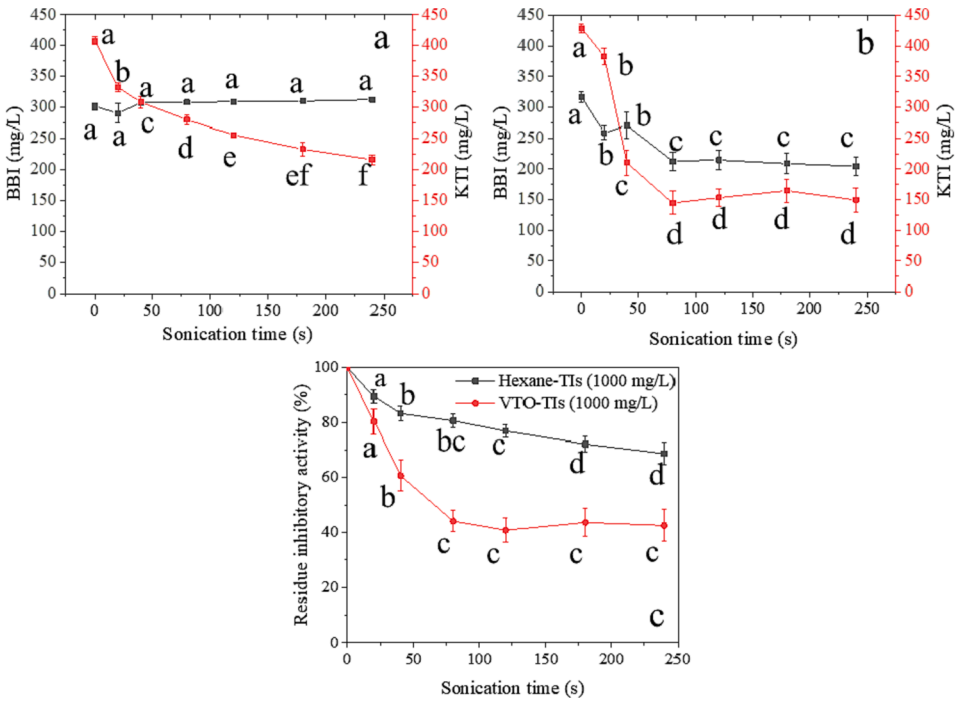

Fig. 3. The residual amount of BBI/KTI in the aqueous phase of hexane-TIs (1000 mg/L, ratio of 1:1 (v:v)) (a) and VTO-TIs (1000 mg/L, ratio of 1:1 (v:v)) emulsions (b) generated over different sonication times. The corresponding residual inhibitory activity (c) of TIs in the aqueous phase of hexane-TIs and VTO-TIs emulsions. Note: BBI: Bowman-Birk inhibitor; KTI: Kunitz inhibitor; TIs: trypsin inhibitors (mixture of BBI and KTI); VTO: vegetable oil. Different lowercase letters represent significant differences in the residual amount or inhibitory activity at different sonication times ($p < 0.05$). The experiments were conducted in triplicate.

at 37 °C for 10 min. Next, 0.5 mL of substrate solution was added before incubating for 10 min at 37 °C. 0.1 mL of 30 % acetic acid was then added to arrest the reaction. The reagent blank was prepared by adding 0.1 mL of 30 % acetic acid to a tube containing 0.2 mL trypsin solution and 0.2 mL deionised water before 0.5 mL of substrate solution was added. The reaction mixture was pipetted (200 μL) into microplate wells (96-well, flat-bottom, Greiner Bio-One) and the absorbance at 410 nm was measured using a microplate reader (SPECTROstar Nano, BMG Labtech). One trypsin unit is defined as an increase of 0.01 absorbance units at 410 nm and trypsin inhibitor activity is expressed as trypsin units inhibited [34].

2.4.3. SDS-Page

SDS-PAGE was carried out to identify the formation of intermolecular interaction of TI molecules (e.g., C—C bonds, S—S bonds) that could be related to conformational changes of desorbed KTI and BBI [8]. Briefly, 1000 mg/L of initial and desorbed KTI and BBI samples were mixed with Laemmli sample buffer (non-reducing SDS-PAGE) or sample buffer with 5 % mercaptoethanol (reducing SDS-PAGE) at a ratio of 1:1 (v:v). Then the mixture was heated at 90 °C for 5 min to unfold the tertiary structure of TIs. 30 μL of sample or protein standard was pipetted into the gel lanes of the Criterion™ TGX™ Precast PAGE Gels. Around 400 mL of Tris/glycine/SDS running buffer was added and the gel was run at 200 V for 40 min. After running, the gel was stained with Coomassie Biosafe stain for 1 h following a de-staining using deionised water for 1 h. The image of the de-stained gel was acquired using a Bio-Safe Gel-Doc (Bio-Rad).

2.4.4. Particle size of BBI and KTI

To clarify whether the interfacial adsorption of KTI and BBI could lead to intermolecular aggregation, the average size of untreated BBI/KTI and desorbed BBI/KTI were measured by dynamic light scattering (DLS, Zetasizer Nano, Malvern Analytical ltd, Malvern, UK) equipped with a 633-nm laser at 25 °C [10].

2.4.5. Confocal laser scanning microscopy

To observe the microstructure of desorbed BBI and KTI, a Leica SP8 confocal microscope (Leica Microsystems, Wetzlar, Germany) was employed. For this, untreated and desorbed KTI and BBI (dyed with Fast green) from the hexane-water interface were transferred onto microscope glass slides and covered with a coverslip. Fast green dye was excited at 633 nm using Ar and He–Ne laser lines. The fluorescence emission was captured through a 60 × lens using 2 photomultiplier tubes set at 655–755.

2.4.6. Circular dichroism spectroscopy and fluorescence spectrum

Potential changes in the secondary and tertiary structure of KTI and BBI desorbed from the hexane-water interface were also examined using circular dichroism and fluorescence spectroscopy, respectively. For the analysis of the secondary structure [10], desorbed KTI and BBI solutions (obtained as previously described in section 2.5) and original KTI and BBI solutions were diluted to 200 mg/L and then pipetted into a quartz cell with 1 mm path length. The wavelength was scanned from 260 nm to 190 nm with a scanning speed of 50 nm/min and a bandwidth of 1 nm using circular dichroism spectroscopy (Mode J-815, JASCO Inc., Japan). Each circular dichroism spectrogram was the average of three spectra accumulations. α-helix, β-sheet, β-turn and random coil were acquired using Protein Secondary Structure Estimation Software of Spectra Manager (JASCO Inc., Japan).

For the measurement of tertiary structure [10], emission fluorescence spectroscopy was performed on the original and desorbed KTI and BBI solutions using an Agilent Cary Eclipse fluorescence spectrophotometer (Agilent Technologies, Inc, USA). The excitation wavelength was fixed at 280 nm and the emission wavelength was measured from 290 nm to 450 nm. In addition, the slit widths of excitation and emission were fixed at 5 nm for all measurements.

2.5. The physicochemical properties of emulsions

2.5.1. Optical and fluorescence microscopy

The microstructure of TI emulsions was observed using optical and fluorescence images according to the method of Zhu et al. [35]. Optical microscopy was performed using an inverted Olympus microscope equipped with 10 × and 60 × objective lenses (Model IX7, Australia). To obtain fluorescence images, Nile red (20 mg/L) was added to the hexane before the preparation of emulsion. Then the Nile red-dyed hexane was

mixed with the TI solution using handshaking, rotor–stator mixing or ultrasonication to produce an emulsion for subsequent microscopic observation.

2.5.2. Emulsion size distribution and average emulsion droplet size

The particle size distribution and the average size of droplets in the emulsion layer were measured to compare the emulsion stability and surface area following the method described by Zembyla et al. [36] using a Malvern Mastersizer 3000 with a Hydro EV accessory (Malvern Panalytical ltd, Malvern, UK). The emulsion layer was added into the sample loading container to within an obscuration range of 2 % to 10 % to avoid multiple scattering [37]. The refractive indices of water, hexane and VTO were set as 1.33, 1.37 and 1.47, respectively. The absorption index of 0.001 was applied. The average emulsion droplet size and the emulsion layer volume were recorded to calculate the interfacial area.

2.5.3. Interfacial tension measurement

To understand the effect of different non-aqueous phase materials on the adsorption of TIs at a liquid–liquid interface, an optical tensiometer (OCA20, DataPhysics Instruments Co., Germany) was employed to measure the water-hexane and water-VTO interfacial tension in the presence of TIs [38]. For this, a drop of TI solution (1000 mg/L) was injected into the hexane- or VTO-loaded rectangular cuvette. Then an image of the pendant drop was simultaneously captured by a digital camera to record the shape to calculate the real-time interfacial tension using the Young-Laplace equation. The data points were collected manually within the first 30 s and then switched to automatic acquisition at a rate of 1 datapoint every 6 s.

2.6. Statistical analyses

All treatments and analyses were conducted in triplicate. The data are presented as the mean ± SD values. Minitab 18 software was used to analyse the data. One-way ANOVA test and Fisher's test (at 5 % level of probability, $p < 0.05$) were used to evaluate the statistical differences among means.

3. Results and discussion

3.1. Comparison of hand shaking, rotor–stator mixing and ultrasound mixing on the hexane-water interfacial adsorption and inactivation of TIs

To investigate the feasibility of the inactivation of TIs using the liquid–liquid interfacial adsorption method, emulsification of TI solution was applied to generate the liquid–liquid interface. In addition, considering the concentration of TIs in the actual food system [39,40], the initial TI concentration for emulsification was set from 200 mg/L to 1000 mg/L. Hexane as the common solvent in the food industry has been applied to investigate the adsorption behaviour of proteins [28]. Furthermore, the adsorbed TI molecules can be easily recovered from the hexane interface due to the highly volatile. Accordingly, the immiscible liquids consisting of hexane and TI solution were first chosen as the theoretical model to measure the adsorbed amount of KTI and BBI at the droplet interface and the residue inhibitory activity of TIs after removing the hexane-aqueous interface. Three different emulsification methods (HS, UT and US) were employed to compare their capacity on the generation of emulsion droplets, adsorption amount of TIs and inactivation efficiency of TIs.

The microstructure of emulsion droplets generated by HS, UT and US was presented in SI Fig. 1. It can be seen that emulsions prepared by US had a higher droplet population and smaller size. For example, the emulsion produced by HS obviously demonstrated larger emulsion droplets (around 100 μm) due to flocculation and an uneven droplet size distribution. In contrast, the UT emulsification of hexane-TIs presented smaller emulsion droplets (around 50 μm) and exhibited fewer large emulsion droplets. After US treatment of hexane-TI solution mixture, the formation of the smallest emulsion droplet (<20 μm) and more uniform size distribution can be observed. The different performances of the abovementioned emulsification methods on the generation of droplet size may be explained by their different turbulent intensity [29]. Generally, the turbulent intensity is calculated according to the Kolmogorov length scale (i.e., energy dissipation rate estimation) regardless of the total energy input. Li et al. [41] reported that the estimated turbulent intensity of low-frequency US (20 kHz) was 100-fold higher (4.4×10^{8} W/kg) than that of UT when their energy input was same, which resulted in a smaller turbulent eddy size of during ultrasonication.

Although the emulsion can be successfully produced by selected emulsification methods, the adsorption amount and residue activity of TIs is still required as the direct evidence to verify the proposed interfacial adsorption-induced TI inactivation method. The unadsorbed amount of BBI and KTI and the residue inhibitory activity of TIs on hexane-TI emulsions generated by HS, UT and US mixing are presented in Fig. 1. For HS emulsification, almost all of the KTI and BBI remained in the aqueous phase rather than adsorbing at the hexane-water interface without significant decrease in the activity, at all investigated TI concentrations ($p \geq 0.05$). In comparison, UT showed a stronger capacity to enhance the adsorption of TIs at the low TI concentration (200 mg/L), especially for KTI. For instance, around 20 % of KTI was adsorbed at the interface after UT emulsification which contributed to approximately 10 % loss of TI activity when the TI concentration was 200 mg/L. Despite this, UT mixing presented obviously low efficiency when the TI concentration increased to over 500 mg/L ($p \geq 0.05$). Although all selected emulsification methods have limited influence on the adsorption of BBI. However, compared with HS or UT emulsification, US emulsification method has the highest potential on the adsorption and inactivation of KTI, particularly for the high TI concentration (>500 mg/L). For instance, the adsorption amount of KTI was 80 mg/L at the TI concentration of 1000 mg/L resulting in a 19 % reduction in the TI activity. This result is consistent with the emulsion droplet size generated by HS, UT and US, which the emulsion with a smaller droplet size can generate more interface for TI adsorption and inactivation. However, it is still unclear about the reason and influencing factors of the adsorption behaviour of KTI and BBI at the emulsion droplet interface. On the other hand, it should be noticed that 30 min low-frequency sonication (20 kHz, 1.28 W/mL) was required to inactivate 84 mg/L of KTI at a TI initial concentration of 1000 mg/L according to the report of Wu et al. [10], which the sonication time is 90-fold longer than the US-assisted emulsification time. Therefore, the reduction and inactivation of TIs in this study was caused by interfacial adsorption rather than US. Based on the satisfactory performance, US was selected to further investigate the effect of non-aqueous phase and ultrasonic time on the TI adsorption at emulsion droplet interface.

3.2. The effect of non-aqueous phase on the US-assisted interfacial adsorption kinetics of TIs

3.2.1. The microstructure and interfacial area of hexane-TIs and VTO-TIs emulsions generated over different ultrasonication times

Generally, emulsification depends on the interfacial properties and the energy transferred to a liquid–liquid system, which can be related to the properties of the non-aqueous phase and to the ultrasonication time [24]. In contrast to hexane, VTO is involved in the production of practical food-related products (e.g., emulsions and gels), which can provide a guidance for the feasibility of US-assisted interfacial adsorption and inactivation of TIs in actual food system. Images of hexane-TI (1000 mg/L) and VTO-TI (1000 mg/L) emulsions prepared over different ultrasonication times (20 s-240 s) are presented in SI Fig. 4 and their optical microscopy images and size distribution are shown in Fig. 2**a**. The emulsions of hexane-TIs prepared by US exhibited bimodal particle distributions at shorter sonication times, and became increasingly monomodal following longer treatments. In comparison, the droplets of VTO-TIs emulsions appeared to have overlapping bimodal distributions.

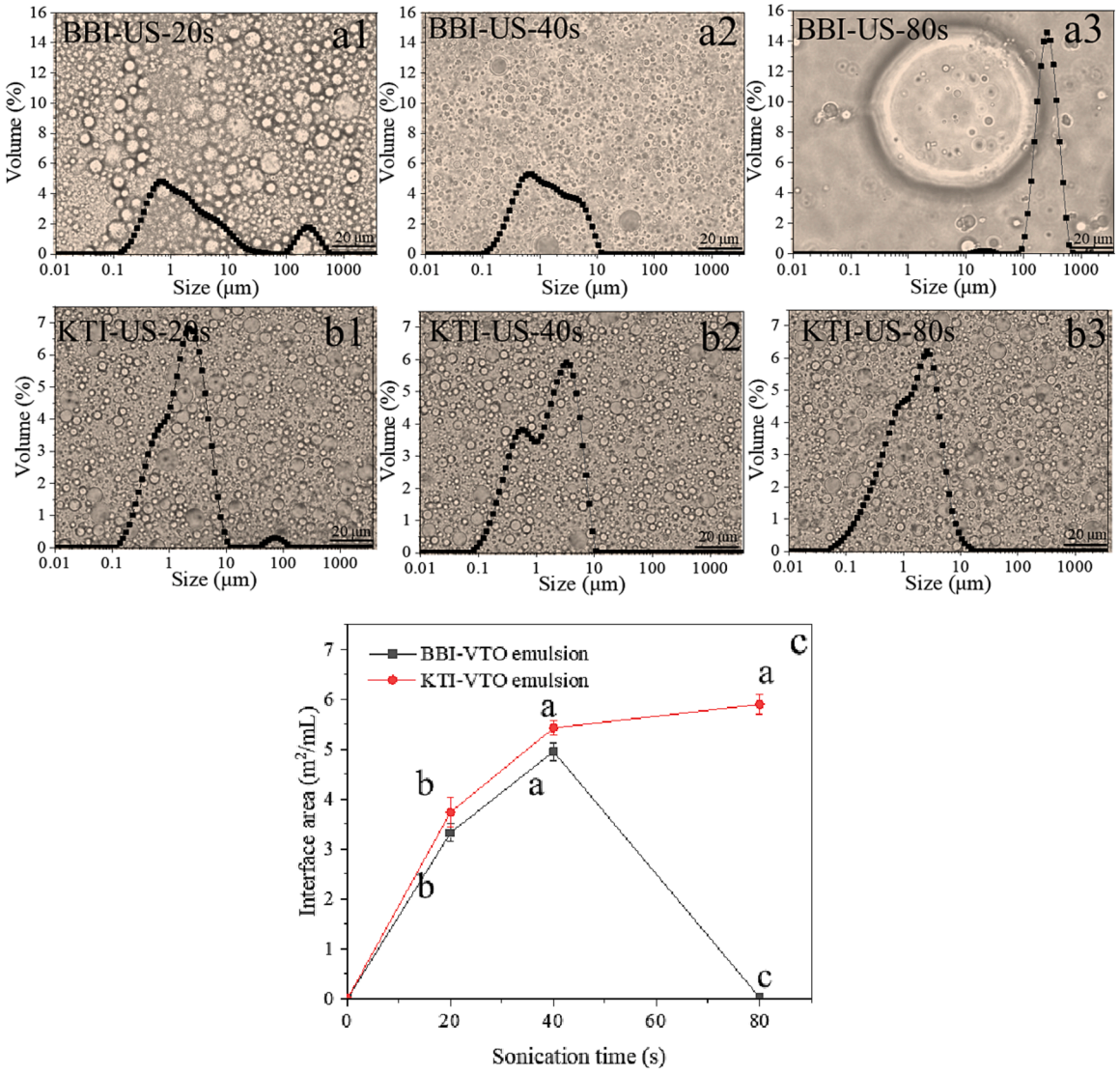

Fig. 4. Optical microscopic images (60 ×) and corresponding size distributions of BBI-VTO (500 mg/L, ratio of 1:1 (v:v)) (a) and KTI-VTO (500 mg/L, ratio of 1:1 (v:v)) (b) emulsions generated by ultrasound at 1.28 W/mL for 20 s-80 s. The corresponding interfacial area of BBI-VTO and KTI-VTO emulsion (c). Note: BBI: Bowman-Birk inhibitor; KTI: Kunitz inhibitor; VTO: vegetable oil. Different lowercase letters represent significant differences in the surface area at different sonication times ($p < 0.05$). The experiments were conducted in triplicate.

In addition, the emulsion droplets were generally smaller in the VTO-TI emulsions (1–10 μm) than the hexane-TIs (5–100 μm) (Fig. 2**c**). As a result, the VTO emulsions had considerably higher total interfacial area due to the decreased droplet size. For example, the estimated total surface area (based on the volume and droplet size of emulsion layer) of VTO-TIs emulsion droplets was approximately 3.31 m^2/g compared to 0.34 m^2/g for the hexane-TIs emulsion after sonication for 20 s. In addition to the increased surface area, smaller droplets and narrower droplet size distributions are associated with more stable emulsions [42]. Accordingly, VTO had better performance on the stability of emulsion and the generation of droplet interface area, which may benefit the adsorption process of TIs at the water–oil interface.

To further explore the reason that VTO as non-aqueous phase has better performance on the generation of TI emulsions, the dynamic interfacial tension of TIs (1000 mg/L) at the hexane and VTO liquids was measured (Fig. 2**d**). The initial interfacial tension of TIs in hexane was around 37 mN/m while that of TIs in VTO was 2-fold lower (16.9 mN/m). In addition, the TIs at hexane and VTO presented different reduction trends in interfacial tension with the increased time. Generally, the formation (i.e., break-up and coalescence) of emulsion droplets highly depends on the turbulence energy, interfacial energy and viscosity [43–45]. It has been reported that the break-up rate of droplets decreased from around 70 s^{-1} to<10 s^{-1} when the interfacial tension increased from 1 mN/m to 30 mN/m [45]. This could be the reason to explain the smaller droplet size and higher surface area observed in the ultrasonic emulsification of VTO-TIs.

3.2.2. The adsorption amount and residue inhibitory activity of TIs in hexane-TIs and VTO-TIs emulsions

To further verify whether the increased surface area of emulsion droplets can benefit the adsorption and inactivation procedure, the adsorption amount of BBI/KTI and residual inhibitory activity of TIs were investigated and are presented in Fig. 3. For the ultrasonic emulsification of hexane-TIs, the residual amount of KTI in the aqueous phase was continuously decreased by around 50 % during 240 s sonication, while that of BBI was insignificantly changed (Fig. 3**b**). In comparison, both the residual amount of KTI and BBI in the aqueous phase experienced an obviously decline within the first 80 s sonication and then plateaued in the ultrasonic emulsification of VTO-TIs. Specifically, around 70 % of KTI and 30 % of BBI were adsorbed at the water-VTO

interface after sonication for 240 s. This result is consistent with the generation of larger emulsion surface area in the VTO-TI emulsion enabling more interfacial adsorption of TIs. In addition, the residual inhibitory activity of TIs directly reflected the inactivation efficiency of interface-induced inactivation. As shown in Fig. 3**c**, the residual inhibitory activity of TIs in the aqueous phase from ultrasonic emulsification of hexane-TIs experienced a continuously decreasing trend with the increase of sonication time from 20 s to 240 s. Differently, the inhibitory activity of TIs in the VTO-TIs emulsion generated by ultrasound was first decreased to around 40 % and then plateaued. Apart from the shorter equilibrium time, the residual inhibitory activity of TIs from the VTO-TIs emulsion was around half that in the hexane-TIs emulsion. This indicates that using VTO as the non-aqueous phase and applying longer sonication times can benefit the inactivation procedure of TIs by providing more interfacial surface for adsorption. However, it is still unclear whether the decreased TI activity was contributed by the inactivation of adsorbed BBI, KTI or both. Also, the exact inactivation mechanism of BBI and KTI at liquid–liquid interface is not resolved.

3.3. US-assisted interface-induced inactivation on individual BBI or KTI systems

3.3.1. The microstructure and interfacial area of BBI and KTI emulsions

To clarify the adsorption and inactivation behaviours of KTI and BBI at the liquid–liquid interface, BBI and KTI standard solutions (500 mg/L) were applied for the US-assisted interface adsorption separately. The microstructures and size distributions of BBI-VTO and KTI-VTO emulsions during sonication at 1.28 W/mL for 80 s are presented in Fig. 4**a and 4b**. For the ultrasonic emulsification of BBI (Fig. 4**a**), the emulsion droplets shifted from the bimodal particle distributions to the monomodal distribution when the sonication time was increased from 20 s to 40 s. However, the further increase in the sonication time contributed to the phase inversion of BBI emulsion (from O/W to W/O), which reduced the emulsion volume and increased the droplet size (SI Fig. 5 and SI Fig. 6). To further verify the phase inversion in BBI emulsions, the ultrasonic emulsification time was increased to 240 s and the same phenomenon can be still observed (SI Fig. 7). As a result, a significant shift in the interfacial area of BBI emulsion can be found, with a decrease from over 4 m^2/mL to<0.2 m^2/mL when the ultrasonic time was increased from 40 s to 80 s. Differently, the KTI emulsion obtained from ultrasonic emulsification was more stable without obvious coalescence or phase inversion. Consequently, the calculated surface area of KTI emulsion was significantly higher than that of the BBI emulsion after 80 s of sonication (Fig. 4**c**). Generally, the catastrophic phase inversion is triggered by high turbulence intensity such as US [43]. However, the phase inversion of the emulsion could also be related to the emulsifier properties [46–48]. Interfacial rearrangement could reduce system entropy, surface free energy, wetting angle and maintain droplet curvature which make the system more stable [43,46–48]. In comparison, proteins with higher stability cannot contribute to the interfacial energy reduction, which is more likely to trigger phase inversion due to the higher wetting angle [43,46–48]. Accordingly, the different stability of BBI and KTI emulsions may be related to their structural properties since the ultrasonic condition and initial non-aqueous phase fraction were the same during ultrasonic emulsification. The specific structural change of KTI and BBI on the interfacial surface was clarified in the later section.

3.3.2. Adsorption amount and residue inhibitory activity of BBI and KIT

To clarify whether the abovementioned differences in the interfacial areas of BBI and KTI emulsions is related to their different adsorption and inactivation behaviour, their adsorption amount and residual inhibitory activity were compared. As shown in Fig. 5**a**, the residual amount of KTI was decreased by 80% following ultrasonic emulsification for 40 s and then remained at this level over further ultrasonication. This trend was similar to the change in residual activity, implying that the adsorption of KTI at the liquid–liquid interface contributes directly to its inactivation. Contrarily, the residual amount and activity of BBI showed a decreasing trend after ultrasonic emulsification for 40 s. With prolonged sonication (>40 s), both the residual amount and activity of BBI were significantly increased (Fig. 5**b**). In addition, RP-HPLC spectra showed that the retention time and peak shape of emulsions of BBI sonicated for 80 s were similar to a non-sonicated emulsion (SI Figure 8). It has been proposed that US can help desorb colloidal particles from the interfaces of emulsions and foams and such desorption behaviour depends on the properties of particles [49]. Therefore, the minor change in both peak area and retention time of BBI after ultrasonic emulsification for 80 s may be related to the US-induced desorption of BBI from the interface due to the instability of the emulsion. This result is consistent with the aggregation and coalescence of emulsion droplets observed in ultrasonic emulsification of BBI for 80 s. These results further confirm the positive association between the interfacial area of the emulsion and the adsorption amount/residue activity of BBI/KTI. However, it is still unknown about the relationship between the adsorption and inactivation behaviours of BBI and KTI at the liquid–liquid interface.

3.3.3. Conformational changes in BBI and KTI at the liquid–liquid interface

To clarify the pathway of interface-induced inactivation of TIs, the BBI and KTI were first adsorbed at the hexane-water interface and then desorbed from the interface by freeze-drying. The particle size of original BBI/KTI and desorbed BBI/KTI were first compared. As shown in Fig. 6**b**, the average size of untreated BBI and KTI were both around 5 nm. After adsorption and desorption from the hexane-water interface,

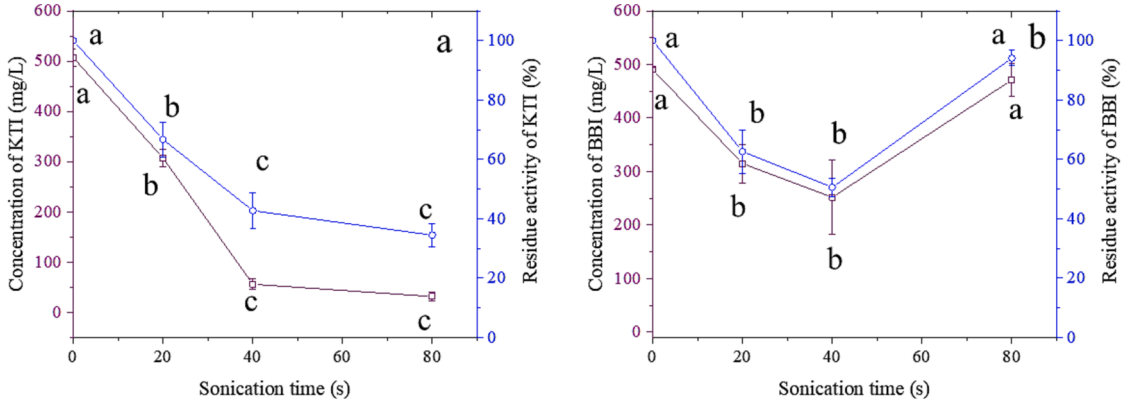

Fig. 5. The residual amount and residual activity of KTI (a) and BBI (b) in aqueous phase during ultrasonic emulsification for 80 s. Note: BBI: Bowman-Birk inhibitor; KTI: Kunitz inhibitor. Different lowercase letters represent significant differences among emulsions treated for different sonication times ($p < 0.05$). The experiments were conducted in triplicate.

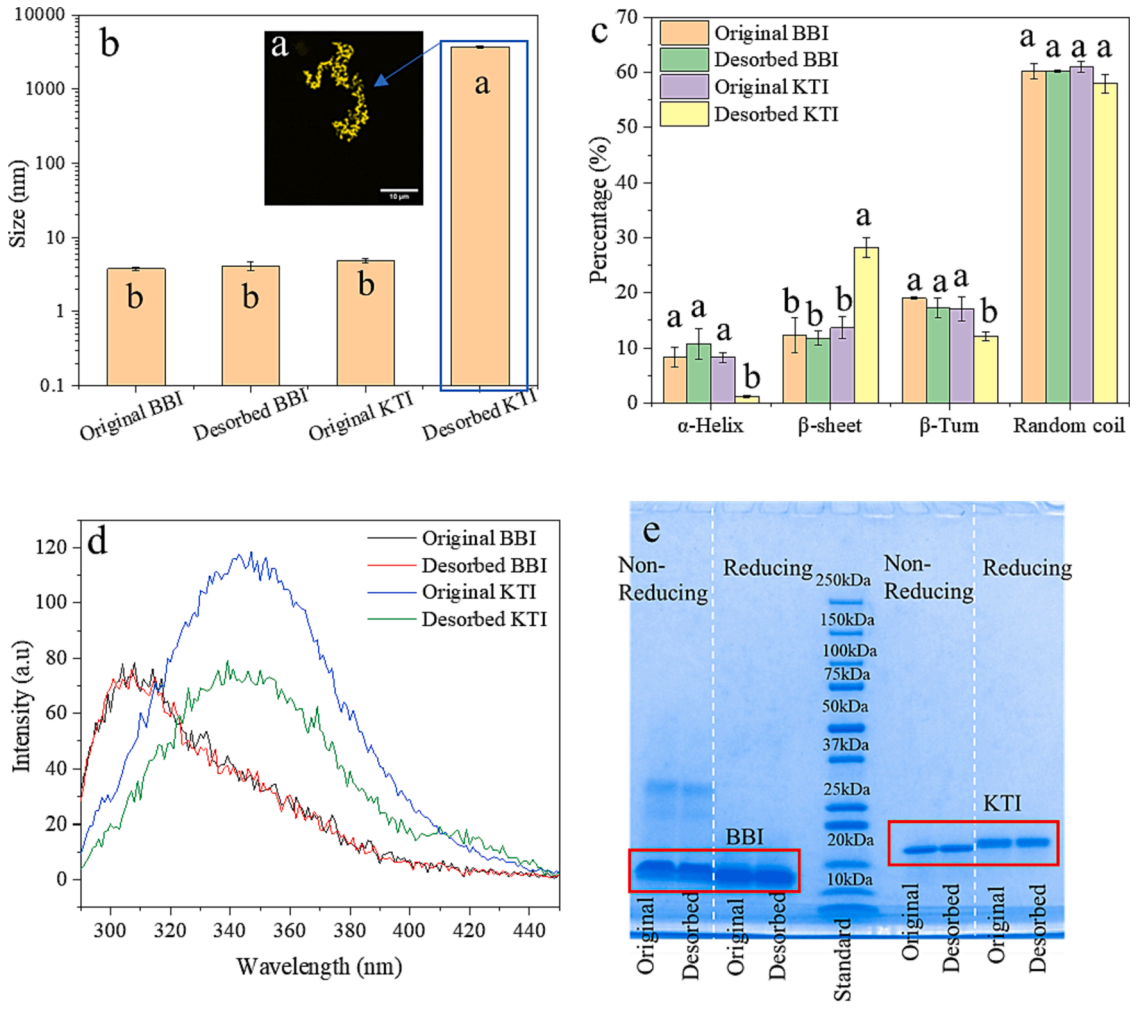

Fig. 6. Confocal images of desorbed KTI (a). The average size of original BBI, original KTI, desorbed BBI and desorbed KTI (b). The secondary structure (c), intrinsic fluorescence spectra (d) and SDS-PAGE images (e) of original BBI, original KTI, desorbed BBI and desorbed KTI. Note: BBI: Bowman-Birk inhibitor; KTI: Kunitz inhibitor. The experiments were conducted in triplicate.

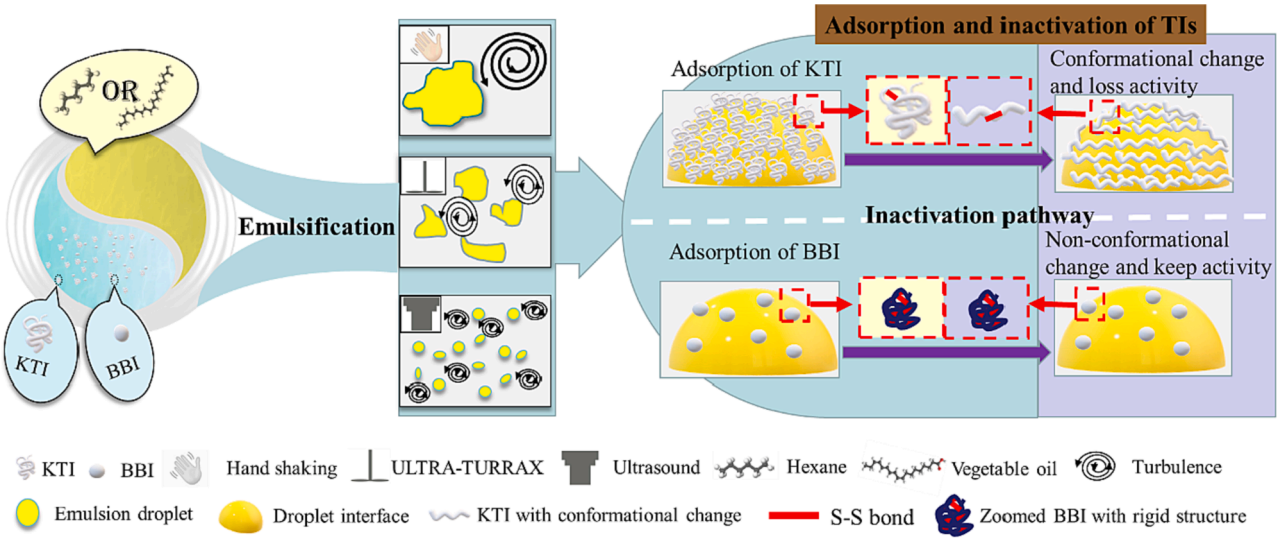

Fig. 7. Schematic illustration of the interfacial adsorption-induced inactivation mechanism of TIs. TI emulsion formulation factors including non-aqueous phase type (e.g., hexane and VTO) and emulsification methods (e.g., hand shaking, ULTRA-TURRAX mixing and ultrasound mixing) were shown to be central to the emulsion droplet surface area. The BBI and KTI are related to the stabilization of liquid–liquid interfaces. The conformational change of KTI at the droplet interface caused the loss of its activity while highly stability of BBI at the interface kept its biological activity.

the average size of KTI was significantly increased to over 1000 nm with an observable aggregation using confocal microscopy (Fig. 6**a**). However, there was only a very minor change in the particle size of BBI ($p \geq 0.05$) following desorption, indicating the different behaviour of KTI and BBI at the liquid–liquid interface. Generally, the adsorption of proteins at a liquid–liquid interface can be classified into two stages [50]. In the first stage, the proteins can migrate and attach to the liquid–liquid interface due to their hydrophilicity and hydrophobicity. In the second stage, the structural rearrangement of adsorbed proteins allows them to form a viscoelastic film at the interfacial layer, which can stabilize the emulsion droplets via steric hindrance and electrostatic repulsion. Therefore, abovementioned different size of desorbed BBI and KTI may be related to the different adsorption behaviour at the second stage.

To verify whether the different aggregation degree of desorbed BBI and KTI is associated with their structural rearrangement at liquid–liquid interface, the secondary and tertiary structure of desorbed BBI and KTI were further compared with their original form. Compared with untreated KTI, the α-helix and β-turn of desorbed KTI was decreased while the β-sheet was significantly increased (Fig. 6**c**). A similar trend was demonstrated by Wong et al. [51], in which the α-helix content of β-casein at an oil–water emulsion interface was decreased while there was an increase in the β-sheet content. Interestingly, the secondary structure of desorbed BBI was not signficantly affected by adsorption at the liquid–liquid interface ($p \geq 0.05$).

The intrinsic fluorescence spectra of original BBI, original KTI, desorbed BBI and desorbed KTI are shown in Fig. 6**d**. Intrinsic fluorescence is mainly generated from tryptophan residues (Trp) and tyrosine residues (Tyr) in TIs, and can reflect changes in the tertiary structure of proteins [52]. The obvious decrease in the fluorescence intensity of desorbed KTI indicates a change in the tertiary structure (Fig. 6**d**) [10]. For BBI, there was no obvious changes in the shift of λ^{max} or the fluorescence intensity, which is consistent with the result of secondary structure. In addition, non-reducing and reducing SDS-PAGE showed that there was no formation of C—C or S—S bond in either the desorbed BBI or KTI (Fig. 6**e**), confirming that the adsorption behaviour did not involve a chemical reaction. The different phenomena of desorbed BBI and KTI may be contributed by their different structural properties. BBI has a rigid (7 disulphide bonds) and compact structure which has been shown to contribute to its high stability in various extreme environments (i.e. extreme thermal, proteolytic and pH) [53]. In contrast, the structure of KTI is more flexible due to fewer disulphide bonds (2 disulphide bonds) [54]. Accordingly, it can be proposed that although BBI can be partly adsorbed at the liquid–liquid interface, it is still quite stable during adsorption processing without significant conformational changes.

3.4. Proposed mechanism of interfacial adsorption-induced inactivation of KTI and BBI

Based on the aforementioned results, the mechanism of interfacial adsorption-induced inactivation of TIs can be proposed. Initially, three different emulsification methods with different turbulent intensities (US > UT > HS) were applied to a model TI emulsion (hexane as non-aqueous phase) to verify the feasibility of the TIs inactivation via liquid–liquid interfacial adsorption [22,40]. As a result, the stronger turbulent intensity (US) helped generate more homogenous and smaller droplets to provide more droplet interface for TI adsorption. Interestingly, KTI showed greater potential for the adsorption at the emulsion droplet interface compared to BBI.

To continuously explore the effect of non-aqueous phase on the interfacial adsorption-induced inactivation of TIs, VTO was selected as a representative oil phase in a food-related system and US with the best performance on emulsification was applied to assist the creation of the VTO-aqueous interface. Compared with the hexane-water interface, the interfacial tension of TIs at VTO-water interface was lower. Generally, for given energy transferred to the liquid–liquid system, lower interfacial tension benefits the emulsification procedure in which emulsifiers can be more efficiently adsorbed at the water–oil interface to reduce the interfacial tension and produce smaller droplets [55,56]. It has been shown that the droplet size of VTO-water emulsions was significantly smaller than that of hexane-water emulsions. Consequently, the smaller droplet size provides more water–oil interface area for KTI and BBI to adsorb, with a greater enhancement in the adsorption of KTI at the water–oil interface than for BBI. However, the specific reason for the different adsorption behaviour of KTI and BBI at the droplet interface is still unknown at this stage.

Overall, the modification of the abovementioned turbulent intensity and non-aqueous phase has limited influence on the adsorption and inactivation of BBI compared to KTI. To further identify the individual adsorption and inactivation behaviour of BBI and KTI at the liquid interface, individual BBI and KTI systems were investigated. For the adsorption of BBI at the water–oil interface, BBI can be regarded as non-deformable without obvious conformational change and loss of activity. Such a phenomenon may be associated with its compact and rigid structure [7]. In contrast, KTI experienced structural rearrangement involving both the secondary and tertiary structures. These conformational changes of KTI at the water–oil interface caused the significant decrease in its activity. Finally, the water–oil interface adsorption contributed to the inactivation of KTI instead of BBI.

4. Conclusion

In this study, the liquid–liquid interfacial adsorption properties of soy trypsin inhibitors are found to play a significant role in the inactivation of their inhibitory activities. Three different emulsification methods including HS, UT, and US were first investigated. Compared to handshaking and UT, the droplet size range of TI-hexane emulsions prepared by US were found to be more homogenous with smaller droplets due to the higher turbulent intensity generated by acoustic cavitation. The adsorption amount of KTI and BBI of ultrasonic emulsification was significantly higher than that of HS and UT emulsification. Based on this, ultrasonic emulsification was selected to further investigate the effect of interface properties. Two different non-aqueous phases, hexane and VTO, were applied to generate the emulsion droplets for the adsorption of BBI and KTI. The droplet size of VTO emulsions was over 4-fold lower than that of hexane emulsions, which generated more water–oil interface to increase the adsorption amount of BBI and KTI ($p < 0.05$). A study on individual BBI or KTI systems provided detailed information about their adsorption behaviours at liquid–liquid interfaces. For the BBI adsorption, the protein is stable at the interface without detectable conformational changes, which may be associated with its compact and rigid structure. In comparison, both secondary and tertiary structures of adsorbed KTI were altered. Consequently, the US assisted interface adsorption of TIs caused the inactivation of KTI rather than BBI. This work can provide a guidance for the efficient inactivation of KTI in soy processing.

CRediT authorship contribution statement

Yue Wu: Conceptualization, experiments, data analysis, writing. **Wu Li:** Interpretation of results, writing, supervision. **Haiyan Zhu:** Experiments. **Gregory J. O. Martin:** Interpretation of results, writing, supervision. **Muthupandian Ashokkumar:** Interpretation of results, writing, supervision.

Data availability

Data will be made available on request.

Declaration of Competing Interest

The authors declare that they have no known competing financial interests or personal relationships that could have appeared to influence the work reported in this paper.

Acknowledgements

This work is supported by China Scholarship Council-University of Melbourne Research Scholarship.

Appendix A. Supplementary data

Supplementary data to this article can be found online at https://doi.org/10.1016/j.ultsonch.2023.106315.

References:

[1] F. Alavi, L. Chen, Z. Emam-Djomeh, Effect of ultrasound-assisted alkaline treatment on functional property modifications of faba bean protein, Food Chemistry 354 (2021), 129494.
[2] H. Lynch, C. Johnston, C. Wharton, Plant-based diets: Considerations for environmental impact, protein quality, and exercise performance, Nutrients 10 (2018) 1841.
[3] I.C. Ohanenye, F.-G.-C. Ekezie, R.A. Sarteshnizi, R.T. Boachie, C.U. Emenike, X. Sun, I.D. Nwachukwu, C.C. Udenigwe, Legume seed protein digestibility as influenced by traditional and emerging physical processing technologies, Foods 11 (2022) 2299.
[4] K. Liu, Soybean trypsin inhibitor assay: Further improvement of the standard method approved and reapproved by American oil Chemists' Society and American Association of Cereal Chemists International, Journal of the American Oil Chemists' Society 96 (2019) 635–645.
[5] B.H. Vagadia, S.K. Vanga, V. Raghavan, Inactivation methods of soybean trypsin inhibitor–A review, Trends in Food Science & Technology 64 (2017) 115–125.
[6] J. Li, Q. Xiang, X. Liu, T. Ding, X. Zhang, Y. Zhai, Y. Bai, Inactivation of soybean trypsin inhibitor by dielectric-barrier discharge (DBD) plasma, Food Chemistry 232 (2017) 515–522.
[7] R.F. Qi, Z.W. Song, C.W. Chi, Structural features and molecular evolution of Bowman-Birk protease inhibitors and their potential application, Acta biochimica et biophysica Sinica 37 (2005) 283–292.
[8] Y. Wu, W. Li, G.J.O. Martin, M. Ashokkumar, Mechanism of low-frequency and high-frequency ultrasound-induced inactivation of soy trypsin inhibitors, Food Chemistry 360 (2021), 130057.
[9] Z. Xu, Y. Chen, C. Zhang, X. Kong, Y. Hua, The heat-induced protein aggregate correlated with trypsin inhibitor inactivation in soymilk processing, Journal of Agricultural and Food Chemistry 60 (2012) 8012–8019.
[10] Y. Wu, W. Li, E. Colombo, G.J.O. Martin, M. Ashokkumar, Kinetic and mechanistic study of ultrasonic inactivation of Kunitz (KTI) and Bowman-Birk (BBI) inhibitors in relation to process-relevant parameters, Food Chemistry 134129 (2022).
[11] J.C. Andrade, J.M.G. Mandarino, L.E. Kurozawa, E.I. Ida, The effect of thermal treatment of whole soybean flour on the conversion of isoflavones and inactivation of trypsin inhibitors, Food Chemistry 194 (2016) 1095–1101.
[12] C. Van Der Ven, A.M. Matser, R.W. Van den Berg, Inactivation of soybean trypsin inhibitors and lipoxygenase by high-pressure processing, Journal of Agricultural and Food Chemistry 53 (2005) 1087–1092.
[13] Q. Li, L. Huang, Z. Luo, T.M. Tamer, Stability of trypsin inhibitor isolated from potato fruit juice against pH and heating treatment and in vitro gastrointestinal digestion, Food Chemistry 328 (2020), 127152.
[14] D.F. Marruecos, D.K. Schwartz, J.L. Kaar, Impact of surface interactions on protein conformation, Current Opinion in Colloid & Interface Science 38 (2018) 45–55.
[15] Y.F. Yano, Kinetics of protein unfolding at interfaces, Condensed Matter 24 (2012), 503101.
[16] M. Miriani, M. Keerati-u-rai, M. Corredig, S. Iametti, F. Bonomi, Denaturation of soy proteins in solution and at the oil–water interface: A fluorescence study, Food Hydrocolloids 25 (2011) 620–626.
[17] T. Lefèvre, M. Subirade, Formation of intermolecular β-sheet structures: a phenomenon relevant to protein film structure at oil–water interfaces of emulsions, Journal of colloid and Interface Science 263 (2003) 59–67.
[18] J. Bergfreund, P. Bertsch, P. Fischer, Adsorption of proteins to fluid interfaces: Role of the hydrophobic subphase, Journal of Colloid and Interface Science 584 (2021) 411–417.
[19] R. Miller, D.O. Grigoriev, J. Krägel, A.V. Makievski, J. Maldonado-Valderrama, M. Leser, M. Michel, V.B. Fainerman, Experimental studies on the desorption of adsorbed proteins from liquid interfaces, Food Hydrocolloids 19 (2005) 479–483.
[20] D. Wang, K. Wang, L. Zhao, X. Liu, Z. Hu, Fabrication and application of pickering emulsion stabilized by high pressure homogenization modified longan shell nanofiber, Journal of Food Engineering 339 (2023), 111264.
[21] C. Tan, D.J. McClements, Application of advanced emulsion technology in the food industry: A review and critical evaluation, Foods 10 (4) (2021) 812.
[22] W. Li, T.S.H. Leong, M. Ashokkumar, G.J.O. Martin, A study of the effectiveness and energy efficiency of ultrasonic emulsification, In press, Physical Chemistry Chemical Physics, 2018.
[23] S.M. Jafari, Y. He, B. Bhandari, Production of sub-micron emulsions by ultrasound and microfluidization techniques, Journal of Food Engineering 82 (2007) 478–488.
[24] A. Taha, T. Hu, Z. Zhang, A.M. Bakry, I. Khalifa, S. Pan, H. Hu, Effect of different oils and ultrasound emulsification conditions on the physicochemical properties of emulsions stabilized by soy protein isolate, Ultrasonics Sonochemistry 49 (2018) 283–293.
[25] Y. Tao, D. Li, W. Siong Chai, P.L. Show, X. Yang, S. Manickam, G. Xie, Y. Han, Comparison between airborne ultrasound and contact ultrasound to intensify air drying of blackberry: Heat and mass transfer simulation, energy consumption and quality evaluation, Ultrasonics Sonochemistry 72 (2021), 105410.
[26] Y. Tao, P. Wu, Y. Dai, X. Luo, S. Manickam, D. Li, Y. Han, P.L. Show, Bridge between mass transfer behavior and properties of bubbles under two-stage ultrasound-assisted physisorption of polyphenols using macroporous resin, Chemical Engineering Journal 436 (2022), 135158.
[27] W. Ma, J. Wang, X. Xu, L. Qin, C. Wu, M. Du, Ultrasound treatment improved the physicochemical characteristics of cod protein and enhanced the stability of oil-in-water emulsion, Food Research International 121 (2019) 247–256.
[28] A. Dan, R. Wüstneck, J. Krägel, E.V. Aksenenko, V.B. Fainerman, R. Miller, Interfacial adsorption and rheological behavior of β-casein at the water/hexane interface at different pH, Food Hydrocolloids 34 (2014) 193–201.
[29] W. Li, Y. Wu, G.J.O. Martin, M. Ashokkumar, Turbulence-dependent reversible liquid-gel transition of micellar casein-stabilised emulsions, Food Hydrocolloids 131 (2022), 107819.
[30] T.S.H. Leong, M. Zhou, N. Kukan, M. Ashokkumar, G.J.O. Martin, Preparation of water-in-oil-in-water emulsions by low frequency ultrasound using skim milk and sunflower oil, Food Hydrocolloids 63 (2017) 685–695.
[31] A. Shanmugam, M. Ashokkumar, Ultrasonic preparation of food emulsions, Ultrasound in Food Processing (2017) 287–310.
[32] Q. Zhao, Z. Long, J. Kong, T. Liu, D. Sun-Waterhouse, M. Zhao, Sodium caseinate/flaxseed gum interactions at oil–water interface: Effect on protein adsorption and functions in oil-in-water emulsion, Food Hydrocolloids 43 (2015) 137–145.
[33] E.B.A. Hinderink, L. Sagis, K. Schroën, C.C. Berton-Carabin, Sequential adsorption and interfacial displacement in emulsions stabilized with plant-dairy protein blends, Journal of Colloid and Interface Science 583 (2021) 704–713.
[34] M. Kakade, J. Rackis, J. McGhee, G. Puski, Determination of trypsin inhibitor activity of soy products: a collaborative analysis of an improved procedure, (1974).
[35] H. Zhu, S. Mettu, M.A. Rahim, F. Cavalieri, M. Ashokkumar, Insight into the structural, chemical and surface properties of proteins for the efficient ultrasound assisted co-encapsulation and delivery of micronutrients, Food Chemistry 362 (2021), 130236.
[36] M. Zembyla, B.S. Murray, S.J. Radford, A. Sarkar, Water-in-oil Pickering emulsions stabilized by an interfacial complex of water-insoluble polyphenol crystals and protein, Journal of Colloid and Interface Science 548 (2019) 88–99.
[37] C.J. Gamlath, T.S.H. Leong, M. Ashokkumar, G.J.O. Martin, Incorporating whey protein aggregates produced with heat and ultrasound treatment into rennet gels and model non-fat cheese systems, Food Hydrocolloids 109 (2020), 106103.
[38] B. Yatipanthalawa, W. Li, D.R.A. Hill, Z. Trifunovic, M. Ashokkumar, P.J. Scales, G. J.O. Martin, Interplay between interfacial behaviour, cell structure and shear enables biphasic lipid extraction from whole diatom cells (Navicula sp), Journal of Colloid and Interface Science 589 (2021) 65–76.
[39] G.S. Gilani, K.A. Cockell, E. Sepehr, Effects of antinutritional factors on protein digestibility and amino acid availability in foods, Journal of AOAC international 88 (3) (2005) 967–987.
[40] M.K. Rasha, A.Y. Gibriel, N.M.H. Rasmy, F.M. Abu-Salem, E.A. Abou-Arab, Influence of legume processing treatments individually or in combination on their trypsin inhibitor and total phenolic contents, Australian Journal of Basic and Applied Sciences 5 (5) (2011) 1310–1322.
[41] W. Li, G.J.O. Martin, M. Ashokkumar, Turbulence-induced formation of emulsion gels, Ultrasonics Sonochemistry 81 (2021), 105847.
[42] L. Zhou, J. Zhang, L. Xing, W. Zhang, Applications and effects of ultrasound assisted emulsification in the production of food emulsions: A review, Trends in Food Science & Technology 110 (2021) 493–512.
[43] C.J. Beverung, C.J. Radke, H.W. Blanch, Protein adsorption at the oil/water interface: characterization of adsorption kinetics by dynamic interfacial tension measurements, Biophysical chemistry 81 (1) (1999) 59–80.
[44] A. Begemann, T. Trummler, E. Trautner, J. Hasslberger, M. Klein, Effect of turbulence intensity and surface tension on the emulsification process and its stationary state—A numerical study, The, Canadian Journal of Chemical Engineering 100 (2022) 3549–3561.
[45] H. Zhou, X. Yu, B. Wang, S. Jing, W. Lan, S. Li, Breakup model of oscillating drops in turbulent flow field, Chemical Engineering Science 247 (2022), 117036.
[46] B. Hu, P. Angeli, O.K. Matar, G.F. Hewitt, Prediction of phase inversion in agitated vessels using a two-region model, Chemical Engineering Science 60 (2005) 3487–3495.
[47] J.M. Maffi, G.R. Meira, D.A. Estenoz, Mechanisms and conditions that affect phase inversion processes: A review, The Canadian Journal of Chemical Engineering 99 (2021) 178–208.
[48] L.Y. Yeo, O.K. Matar, E.S.P. de Ortiz, G.F. Hewitt, Simulation studies of phase inversion in agitated vessels using a Monte Carlo technique, Journal of Colloid and Interface Science 248 (2002) 443–454.
[49] V. Poulichet, V. Garbin, Ultrafast desorption of colloidal particles from fluid interfaces, PNAS 112 (2015) 5932–5937.

[50] T.G. Burger, Y. Zhang, Recent progress in the utilization of pea protein as an emulsifier for food applications, Trends in Food Science & Technology 86 (2019) 25–33.
[51] B.T. Wong, J. Zhai, S.V. Hoffmann, M.-I. Aguilar, M. Augustin, T.J. Wooster, L. Day, Conformational changes to deamidated wheat gliadins and β-casein upon adsorption to oil–water emulsion interfaces, Food Hydrocolloids 27 (2012) 91–101.
[52] D. Kong, C. Quan, Q. Xi, R. Han, S. Koseki, P. Li, Q. Du, Y. Yang, F. Forghani, J. Wang, Study on the quality and myofibrillar protein structure of chicken breasts during thawing of ultrasound-assisted slightly acidic electrolyzed water (SAEW), Ultrasonics Sonochemistry 88 (2022), 106105.
[53] A. Gitlin-Domagalska, A. Maciejewska, D. Dębowski, Bowman-Birk inhibitors: Insights into family of multifunctional proteins and peptides with potential therapeutical applications, Pharmaceuticals (Basel) 13 (2020) 421.
[54] M.J. Mishra, Evolutionary Aspects of the Structural Convergence and Functional Diversification of Kunitz-Domain Inhibitors, Journal of Molecular Evolution 88 (2020) 537–548.
[55] F. Ravera, K. Dziza, E. Santini, L. Cristofolini, L. Liggieri, Emulsification and emulsion stability: The role of the interfacial properties, Advances in Colloid and Interface Science 288 (2021), 102344.
[56] L. Guo, X. Xu, X. Zhang, Z. Chen, R. He, H. Ma, Application of simultaneous ultrasonic curing on pork (Longissimus dorsi): Mass transport of NaCl, physical characteristics, and microstructure, Ultrasonics Sonochemistry 92 (2023), 106267.